Numerical Parametric Study of Floor Heave in Gate Roads Caused by Longwall-Induced Abutment Loading

Mark K. Larson
Bo-Hyun Kim
Centers for Disease Prevention, National Institute
for Occupational Safety and Health, Spokane, Washington

ABSTRACT

Floor heave events in underground mining often happen suddenly and cause risk to workers and equipment. Reducing the risk of floor heave must be addressed in mining layout design. To improve that design one must understand the significant parameters that are correlated to the occurrence of floor heave. To accomplish that goal, researchers from the National Institute for Occupational Safety and Health (NIOSH) completed a numerical study using FLAC3D, taking advantage of its strain softening and ubiquitous joint capabilities to better simulate the floor heave and caving mechanisms involved at an actual mine site.

In the study, two models having different uniform pillar sizes in a three-entry gate road system were used to investigate the effect of pillar size and other parameters on floor heave. In the models, a sandstone layer of various thicknesses was placed in the roof at various distances above the coal seam. The models had a brittle stratum just below the coal seam. All other stratigraphic members were one material, designated "rest of strata." Other model parameters that were varied included sandstone and rest of strata elastic moduli and the friction angle of interfaces at the top and bottom of the coal seam. The coal and immediate floor were ubiquitous joint materials with strain softening, which would better simulate the floor heave failure mechanism. Loading was from the overburden as a result of panel excavation.

Normalized floor heave was negatively correlated with the ratio of average vertical strain of the two pillars of each model's gate road system. To be clear, pillars that were strained nearly equally resulted in higher normalized floor heave than when average vertical pillar strains of a gate road were very different. This measure was represented by a ratio of the higher average vertical pillar strain divided by the lower average vertical pillar strain.

The pillar strain ratio had positive correlation with pillar width, and it had negative correlation with two parameters—the distance of the sandstone above the seam and the modulus of the rock in the overburden other than sandstone.

Overall, modeled excavation of one longwall panel resulted in positive correlation of normalized floor heave to distance of the sandstone above the coal seam and negative correlation with pillar width. This result has implications for optimum design of pillars in gate road systems to minimize floor heave.

BACKGROUND

A field study coordinated with a western coal mining company and National Institute for Occupational Safety and Health (NIOSH) resulted in many measurements and observations of behavior of the roof, ribs, and floor of a coal mine (Larson, Tesarik, and Johnson, 2020a). Among the mechanisms documented were roof failure, rib failure, floor heave, and coal bump events. Only one of the bumps was documented in the report by NIOSH (Larson, Tesarik, and Johnson, 2020a). Floor heave is the subject of this report because subsequent modeling did not provide a reasonable explanation for the cause of the floor heave. In that modeling study, the same set of properties between models using Mohr–Coulomb strength criteria and interfaces could not explain the differences in floor heave observed unless a significantly weaker interface was used in the model with the larger pillars. Conventional strength criteria, it seemed, were not adequate to describe the mechanics, and it appeared that use of a more refined mechanical model was required.

A review of constitutive model development is necessary to bring the reader to the current study. NIOSH became aware of the work of Itasca in developing a caving model for cases of block caving mines (Board and Pierce, 2009). Board and Pierce developed for NIOSH a similar caving model for simulating caving in sedimentary rock, which they implemented in what was called the longwall modeling environment (Pierce and Board, 2010a, 2010b). This model was based on Mohr–Coulomb parameter softening of ubiquitous joints in the "subiquitous" (meaning softening-ubiquitous) constitutive model (Itasca, 2009).

Even using this caving model and trying other modeling software, Larson and others found that the behavior they documented at a western U.S. coal mine (Larson, Tesarik, and Johnson, 2020a) could

not be duplicated with Mohr–Coulomb strength models of continua and interfaces without implementing a very weak interface below the immediate floor where floor heave was observed (Larson, Tesarik, and Johnson, 2020b), and a stronger interface where significant floor heave was not observed.

Subsequently, Itasca developed for NIOSH a similar constitutive model that was based on the Hoek–Brown strength criteria and empirical relationships with the Geological Strength Index (GSI) as detailed by Hoek, Carranza-Torres, and Corkum (2002) and named the Cavehoek constitutive model (Garza-Cruz, Pierce, and Lavoie 2012). The Cavehoek model has an option to implement the variable dilation angle as a function of confinement, current friction angle, and accumulated plastic shear strain, as proposed by Alejano and Alonso (2005).

Bo-Hyun Kim joined this research effort and set out to help find an explanation for the floor heave, which seemed to be correlated with larger pillars, not only in this mine, but in two adjacent mines as well. Kim began to apply strain softening of ubiquitous joints and a rough implementation of the S-shaped strength criterion developed by Peter Kaiser and himself (Kaiser and Kim, 2015). An implementation of a spalling model based on the S-shaped strength criterion into Itasca codes was first implemented by Kim, Pierce, and Dzik (2014). Subsequently, it was found that the orientation of the largest compressive principal stress relative to the cleat system affected the degree of strength and brittleness of the behavior of a Utah coal (Kim et al., 2018b; Kim and Larson, 2017, 2018). In a parametric study of developed gate roads using two sizes of pillars, greater floor heave was associated with the larger pillars (Kim and Larson, 2019). The methodology of Kim and Larson took advantage of experimental design methods, also called robust design, developed by Genichi Taguchi (1986). These methods are well described by Phadke (1989). Kim, Larson, and Lawson (2018a) described this method as applied to ground control and demonstrated this method in determining possible risk factors for the occurrence of coal bumps. However, the study by Kim and Larson (2019) did not include loading caused by longwall panel extraction.

As a next step in the initial parametric study of the causes of floor heave (Kim and Larson 2019), the authors used robust design methods in a parametric study of floor heave caused by longwall panel excavation and not just entry development. Such loading is very different and possibly very dependent on stratigraphy.

EXPERIMENTAL DESIGN

Two gate road pillar sizes were modeled using FLAC3D (Figures 1 and 2). Three-entry gate roads with 20-m-wide pillars were simulated as a tailgate, next to a solid barrier pillar. Half of the longwall panel was included in the model, for which the symmetry was not true, but the error would be minimal. Such a simplification was necessary to restrict the size of the model. The model with the larger pillar width (50 m) had a panel excavated on the left of the gate roads, followed by excavation of another panel on the right. For both panels, only half of the excavated panels were included in the model as a simplification. The models were only 2 m in length in the y-direction, and therefore, pseudo-two-dimensional. Zone size near the area of interest was 0.25 m. This size was slightly less than the fine zone size of other models leading up to this study and, therefore, deemed adequate.

The stratigraphy of the mine after which the experiment was somewhat patterned was variable. Even over the first longwall panel, the caving characteristics evolved from caving behind the shields to intact roof bending so that it was in contact with the floor behind the shields. It seemed apparent that a strong, stiff sandstone layer above the coal should be a parameter in this study. A cleat system was employed in a 4-m-thick coal seam. It was assumed that these cleat characteristics transferred into the 4-m-thick immediate floor. This was a reasonable assumption because the floor was very carbonaceous, and the sites studied at the mine were near a fault that caused variation in the orientation of the cleat system. Interfaces were inserted at the top and bottom of the sandstone layer and the coal seam. In addition, the floor heave caused such deformation of floor zones near the ribs that they would trip FLAC3D's bad zone geometry detection threshold resulting from badly deformed zones. Therefore, a routine was written in the script code FISH to check for such an approaching condition. Those zones not meeting the "approaching" geometric ratio threshold were assumed to be rubble and deleted. The deformation of the floor and ribs and the deletion of these "rubble" zones caused a need to define vertical interfaces along each pillar rib, whose interfaces extended into the immediate floor. Such interfaces prevented overlap without mechanical interaction between exposed floor and ribs.

Therefore, independent parameters used in this study were (1) thickness of a strong, stiff sandstone unit in the roof; (2) friction angle of interfaces at the top and bottom of the coal seam; (3) elastic modulus of the sandstone; (4) elastic modulus of the rest of the stratigraphy, excepting the seam, immediate floor, and stiff sandstone; and (5) distance from the seam to the bottom of the sandstone. Although depth of cover affects longwall-induced loading, it was not considered as a parameter so that the study size was manageable.

Each independent parameter was given four levels or values for the modeling parameter study, as listed in Table 1. One could conduct modeling experiments on all possible combinations of these parameters, which would be 4^5, or 1,024, experiments. But according to robust design methods, by using orthogonal arrays of parameters, only 16 experiments needed to be performed so that the results would be statistically equivalent to doing all 1,024 experiments, as listed in Table 2.

The stiff sandstone and the rest of the overburden and strata below the immediate floor were assigned the constitutive model called "subiquitous." This model installs ubiquitous joints at a specified orientation. It includes strain softening along the ubiquitous joints.

The coal and immediate floor zones are assigned the Cavehoek model to simulate the caving process resulting from longwall panel excavation. The model follows the progressive failure and disintegration of the rock mass from an intact/jointed material to a caved material. The creation of the cave results in (1) deformation and stress redistribution of the rock mass above the longwall; (2) failure of the rock mass in advance of the longwall face, with associated progressive reduction in strength from peak to residual levels; and (3) dilation, bulking, fragmentation, and mobilization of caved material. The failure process involves shearing along preexisting joint surfaces and stress-induced fracturing of intact rock blocks. The constitutive model allows for representation of modulus

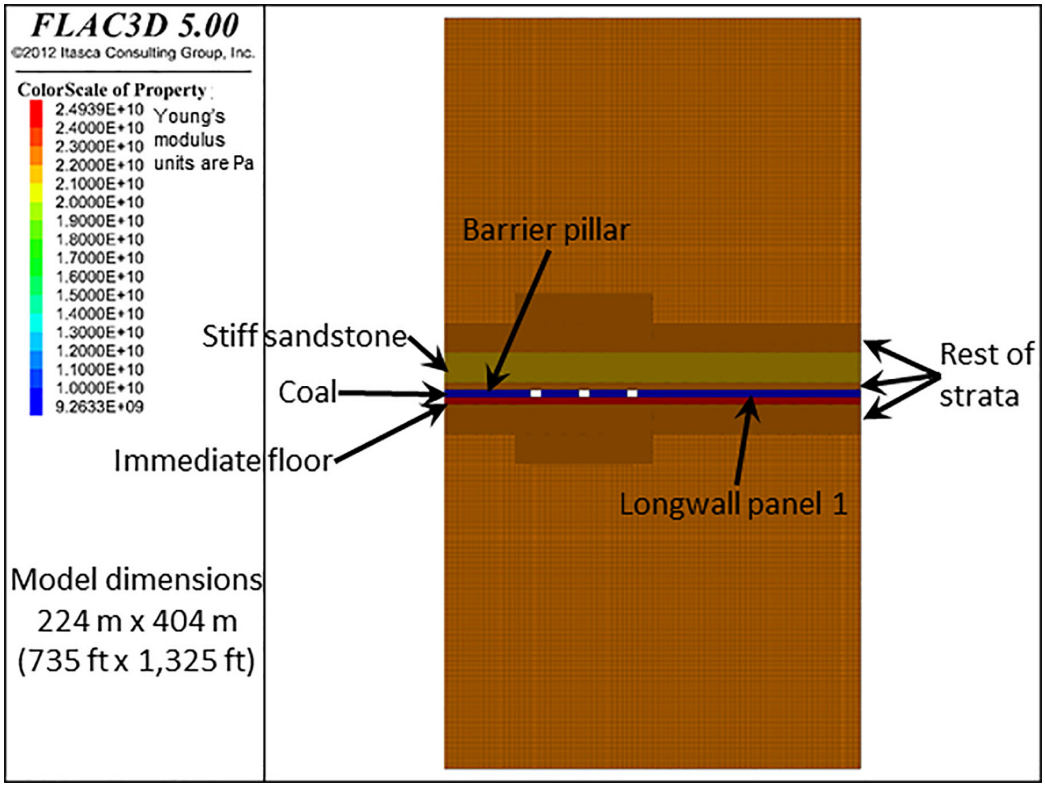

Figure 1. Vertical section of the model with narrow pillars showing by color the rock mass Young's modulus of case 16.

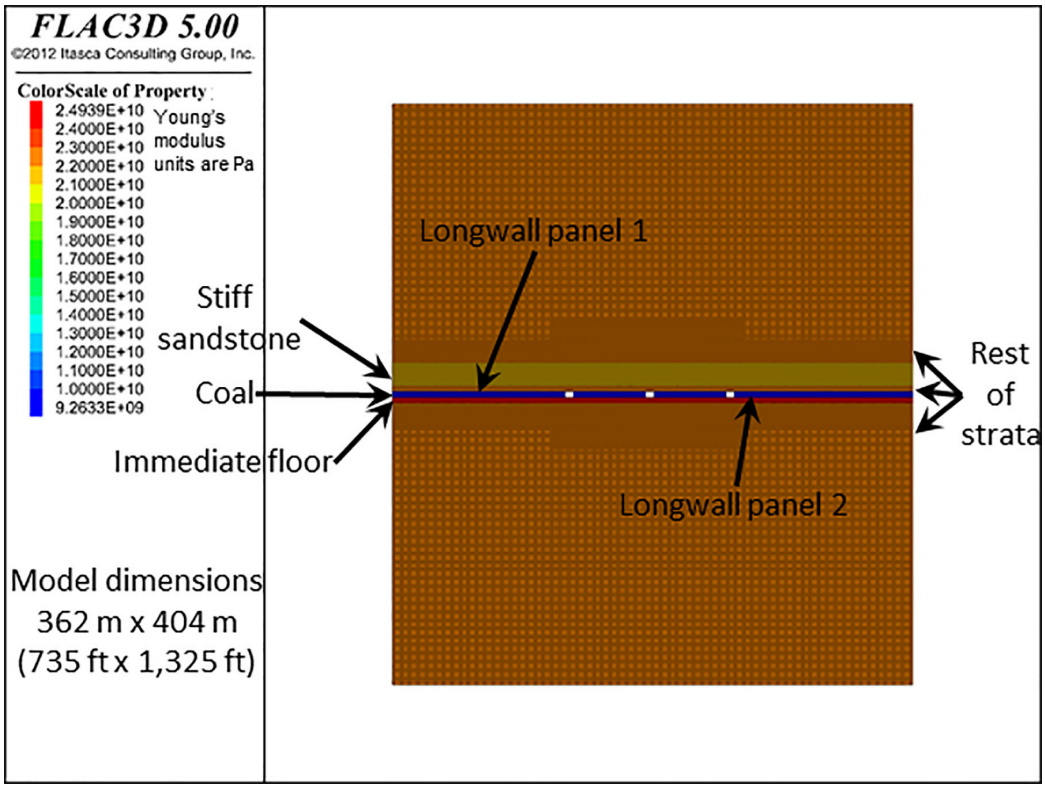

Figure 2. Vertical section of the model with wide pillars showing by color the rock mass Young's modulus of case 16.

Table 1. Levels of independent parameters in the modeling study.

Level	Sandstone Thickness, m (ft)	Friction Angle, °	Sandstone Modulus, GPa (psi)	Rest of Rock Modulus, GPa (psi)	Distance from Coal to Sandstone, m (ft)
1	2 (6.56)	45	33.5867 (4,871,339)	27.6589 (4,011,584)	0 (0)
2	4 (13.12)	50	38.1940 (5,539,571)	35.0001 (5,076,336)	4 (13.12)
3	8 (26.25)	55	51.4147 (7,457,072)	42.3416 (6,141,130)	8 (26.25)
4	16 (52.49)	60	64.2855 (9,323,824)	52.9359 (7,677,704)	16 (52.49)

Table 2. List of orthogonal arrays of the parameters used in the model experiments.

Experiment	Sandstone Thickness, m (ft)	Friction Angle, °	Sandstone Modulus, GPa (psi)	Rest of Rock Modulus, GPa (psi)	Distance from Coal to Sandstone, m (ft)
1	2 (6.56)	45	33.5867 (4,871,339)	27.6589 (4,011,584)	0 (0)
2	2 (6.56)	50	38.1940 (5,539,571)	35.0001 (5,076,336)	4 (13.12)
3	2 (6.56)	55	51.4147 (7,457,072)	42.3416 (6,141,130)	8 (26.25)
4	2 (6.56)	60	64.2855 (9,323,824)	52.9359 (7,677,704)	16 (52.49)
5	4 (13.12)	45	38.1940 (5,539,571)	42.3416 (6,141,130)	16 (52.49)
6	4 (13.12)	50	33.5867 (4,871,339)	52.9359 (7,677,704)	8 (26.25)
7	4 (13.12)	55	64.2855 (9,323,824)	27.6589 (4,011,584)	4 (13.12)
8	4 (13.12)	60	51.4147 (7,457,072)	35.0001 (5,076-336)	0 (0)
9	8 (26.25)	45	51.4147 (7,457,072)	52.9359 (7,677,704)	4 (13.12)
10	8 (26.25)	50	64.2855 (9,323,824)	42.3416 (6,141,130)	0 (0)
11	8 (26.25)	55	33.5867 (4,871,339)	35.0001 (5,076-336)	16 (52.49)
12	8 (26.25)	60	38.1940 (5,539,571)	27.6589 (4,011,584)	8 (26.25)
13	16 (52.49)	45	64.2855 (9,323,824)	35.0001 (5,076-336)	8 (26.25)
14	16 (52.49)	50	51.4147 (7,457,072)	27.6589 (4,011,584)	16 (52.49)
15	16 (52.49)	55	38.1940 (5,539,571)	52.9359 (7,677,704)	0 (0)
16	16 (52.49)	60	33.5867 (4,871,339)	42.3416 (6,141,130)	4 (13.12)

softening, density adjustment, cohesion weakening, and frictional strengthening.

The coal and immediate floor, both 4 m (19.5 ft) in thickness, were given properties listed in Table 3. However, to aid formation of plasticity, the Hoek–Brown parameter, σ_{ci}, was given some variation. Harr (1987) gave some coefficients of variation for several parameters used in civil engineering, for which the coefficient is expressed as a ratio of the standard deviation to the mean. For cohesion, that coefficient was given as 0.40. A similar coefficient of variation should be used for σ_{ci}. It is assumed that the population of σ_{ci} follows a normal distribution. However, limiting the maximum and minimum values of a distribution is necessary in order to stay within a physically plausible range. A normal distribution is approximated with a triangular distribution between 0.6 and 1.4 of the mean. The mean values for σ_{ci} were 42.0 MPa (6,092,000 psi) for coal and 23.0 MPa (3,336,000 psi) for the immediate floor. Admittedly, these values are higher than most coals and sedimentary material floor. However, relative proportions of values among stratigraphic members are what we desired, and results should be similar proportionally to what they would have been with lower values.

The models were built to simulate the approximate geometry of panels, pillars, and entries of a case in the western U.S. (Larson and Whyatt 2012; Larson, Tesarik, and Johnson, 2020a). However, these models were constructed and run using SI units. The 16 cases of Table 2 were each run with narrow pillars of 20-m (65.6-ft) width and with wide pillars of 50-m (164.0-ft) width. These widths compare to 22.3-m (73-ft) and 51.8-m (170-ft) widths in the actual case. Also, in the actual case, the panel 1 width was 245 m (805 ft) and that of panel 2 was 258 m (846 ft). Figure 1 shows an example of the narrow pillar model colored by Young's modulus to show one case of stratigraphy.

Figure 2 shows an example of the wide pillar model with modulus coloring to show the same case of stratigraphy.

Kim and Larson (2019), in their study, used horizontal stress as 3.5 times the overburden weight in the approximate y-direction in the models (perpendicular to the vertical sections) and 2.5 times the overburden weight in the x-direction of the model. Agapito, Gilbride, and Koontz (2005) reported several horizontal stresses measured from overcoring in the region. A recheck of the measurements of Agapito, Gilbride, and Koontz (2005) caused the authors to use different horizontal stresses, even though those

Table 3. Properties of Cavehoek materials in the model.

Strata	Vertical Zone size, m	Vertical Zone Size, ft	Intact Young's Modulus, GPa	Intact Young's Modulus, psi	Poisson's Ratio	GSI
Coal	0.25	0.82	22.6886	3,290,700	0.25	55
Immediate floor	0.25	0.82	34.0324	4,936,000	0.25	70
Strata	m_i	D	m_b	S	a	e_{crit}
Coal	70	0	14.032	0.006738	0.504048	0.225
Immediate floor	12	0	4.110	0.035674	0.501355	0.15

measurements were variable and not always consistent with depth. For these models, the authors assumed $\sigma_{yy} = 1.75 * \sigma_{zz}$ and $\sigma_{xx} = 1.5 * \sigma_{zz}$.

RESULTS

The total volume of material heaved past the original dimensions of the entry was used as an indicator of the amount of floor heave. This volume was determined from the average two-dimensional profile of the heave and given one unit of volume in the y-direction. To lessen the time running the models, when a maximum heave of 0.85 m was detected, then the model calculations were terminated, and the model was stopped and saved. In the cases of the narrow pillar, some runs were run to equilibrium before such a limit was imposed, so that the maximum floor heave sometimes was beyond 0.85 m. Three cases—2, 6, and 7—had such conditions. In an attempt to make the equilibrium profiles of these cases comparable to the others, the floor node with the highest elevation was reduced to 0.85 m. The coordinates of the other floor points were lowered proportionally based on amount of heave.

Floor heave volume was calculated from an average profile across the entry, meaning that heave at roughly the same x-coordinate but with different y-coordinates were averaged together to determine an average heave at that x-coordinate. The average heave profile was then used to determine heave volume using 1-m thickness in the y-dimension.

Table 4 lists the heave volume determined, the adjusted heave for some narrow pillar cases, and floor heave normalized to the maximum case (case 4 of narrow pillars when panel 1 is excavated). Each of these results are either at states of equilibrium or when the maximum heave in the profile reached 0.85 m. Perhaps a better outcome would result from comparison at the same pillar strain or where everything reached equilibrium. However, these results were difficult to achieve. The high degree of deformation caused several zone geometry errors, meaning that the volume of any tetrahedron formed internally in the zone had to be maintained higher than 0.010, as set for this study. In order to aid in keeping zones from reaching that threshold, the following three preventive measures were implemented:

1. Each entry was supported by cable and liner elements in the roof and rib, whose sole purpose was to help prevent geometric errors from badly deformed zones caused by excessive plastic shear deformation. Four wide pillar cases also included support in the floor of entries 1 and 3 because of geometry errors that occurred there after panel excavation.
2. Zones in the floor were put in a memory array for a faster check of zones having a geometric ratio below 0.15. Every 20 calculation steps, a check was made for zones having a geometric ratio below that threshold. If any were identified, they were placed in a zone group until the check was complete. Then, all zones in that group were deleted. The effect is shown with an example in Figure 3.
3. The vertical interfaces along each rib, extending through the immediate floor, were implemented to facilitate interaction between any newly exposed nodes and faces of zones.

The deletion of zones increases the ability of heave, but the deletion of zones actually decreases the volume considered heaved. Thus, there are opposing effects. Because the deleted zones might be considered rubble in the physical case, it is difficult to ascertain how best to handle this potential error. The authors choose to determine heave from the profile without deleted zones because such zones, if not deleted, likely would have bulked in an unrealistic fashion. These zones were assumed to be rubblized, and in an actual mining situation would have been cleaned up with a small scoop.

To determine what parameters influenced floor heave, a multiple linear regression analysis was performed on the results of excavating panel 1 only. Panel 2 results had to be excluded because of the vastly different loading conditions. Initially, all parameters were considered in the analysis. Those results are found in Table 5. The t-value in that table is calculated by dividing the coefficient by its standard error. It is a measure of likelihood that the coefficient is zero. For a larger absolute value of t, it is less likely that the actual value of the parameter could be zero. The t-statistic is compared to the t-distribution for the degrees of freedom. In the t-distribution curve, the area under the curve, represented by being greater than the absolute value of t, represents the probability that the particular coefficient is zero, and therefore not significant. Several parameters are not significant—that is, the probability of that coefficient being zero is greater than 5%. Therefore, subsequent analyses were performed until we arrived at the results shown in Table 6. Stiff sandstone thickness is marginally significant and arguably with little significance. However, it is included as our final analysis because the adjusted r-squared value decreased slightly by excluding it in another multiple linear regression analysis. Therefore, normalized floor heave volume for panel 1 extraction in this study might be represented as

$$\begin{aligned} \textit{Normalized floor heave volume} = {} & 0.89274 \\ & - 0.00617 * \textit{SS\_thick} \\ & + 0.00891 * \textit{Dist\_SS} \\ & - 0.01641 * \textit{Pillar\_width} \end{aligned} \quad \text{(Eq. 1)}$$

Table 4. List of floor heave volume for various cases and panel excavations.

Case	Narrow Cases Panel 1 Heave Volume, m^3 (ft^3)	Narrow Cases Panel 1 Adjusted Heave Volume, m^3 (ft^3)	Normalized Panel 1 Adjusted Heave Volume	Wide Cases Panel 1 Heave Volume, m^3 (ft^3)	Normalized Wide Cases Panel 1 Heave Volume	Wide Cases Panel 2 Heave Volume, m^3 (ft^3)	Normalized Wide Cases Panel 2 Heave Volume
1	2.39 (84.4)	2.39 (84.4)	0.450	0.551 (19.5)	0.104	0.995 (35.1)	0.642
2	3.72 (131)	3.41 (120)*	0.642	0.514 (18.2)	0.097	0.845 (29.8)	0.545
3	3.72 (131)	3.72 (131)	0.701	0.515 (18.2)	0.097	0.941 (33.2)	0.607
4	5.31 (188)	5.31 (188)	**1.000***	0.421 (14.9)	0.079	0.936 (33.1)	0.604
5	3.91 (138)	3.91 (138)	0.737	0.386 (13.6)	0.073	1.000 (35.3)	0.645
6	3.978 (140)	3.29 (116)*	0.620	0.396 (14.0)	0.075	0.874 (30.9)	0.563
7	5.92 (209)	3.11 (110)*	0.5865	0.469 (16.6)	0.088	0.830 (29.3)	0.535
8	2.25 (79.5)	2.25 (79.5)	0.423	0.499 (17.6)	0.094	0.899 (31.7)	0.580
9	2.89 (102)	2.89 (102)	0.543	0.393 (13.9)	0.074	0.717 (25.3)	0.462
10	2.09 (73.8)	2.09 (738)	0.393	0.488 (17.2)	0.092	0.198 (7.00)	0.128
11	2.93 (103)	2.93 (103)	0.553	0.438 (15.5)	0.083	0.995 (35.1)	0.641
12	3.46 (122)	3.46 (122)	0.651	0.566 (20.0)	0.107	0.844 (29.8)	0.544
13	2.52 (89.0)	2.52 (89.0)	0.475	0.517 (18.3)	0.097	0.905 (32.0)	0.583
14	3.247 (115)	3.24 (114)	0.610	0.475 (16.8)	0.090	0.607 (21.4)	0.391
15	1.82 (64.3)	1.82 (64.3)	0.342	0.375 (13.2)	0.071	0.903 (31.9)	0.582
16	3.00 (106)	3.00 (106)	0.566	0.512 (18.1)	0.097	0.977 (34.5)	0.630

* Underlined heave volumes were adjusted to a maximum floor heave of 0.85 m. The case in bold was used to normalize all other results.

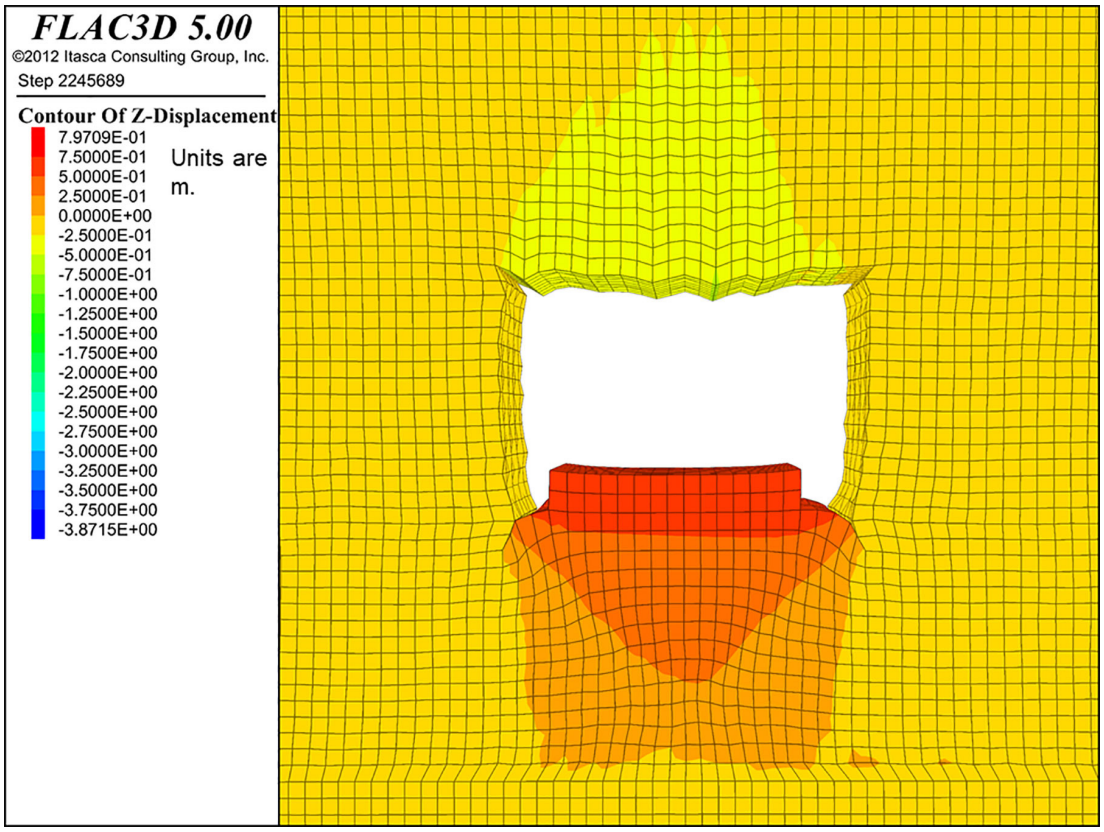

Figure 3. Vertical displacement contours near entry 2 after excavation of both longwall panels.

Table 5. Multiple regression analysis of all parameters for correlation with normalized floor heave resulting from panel 1 excavation.

Parameter	Value	Standard error	t-Value	Probability > |*t*|
Intercept	0.64883	0.19656	3.30094	0.0029
Sandstone thickness	−0.00617	0.0032	−1.92825	0.06526
Interface friction angle	0.00322	0.00307	1.0484	0.30448
Sandstone modulus	7.58461E-7	1.43081E-6	0.53009	0.60072
Rest of strata modulus	9.96923E-7	1.83747E-6	0.54255	0.59224
Distance of sandstone above coal	0.00891	0.0029	3.07002	0.0051
Pillar width	−0.01641	0.00114	−14.33691	1.45E-13

Adjusted r-square value is 0.87366.

Table 6. Multiple regression analysis of selected parameters for correlation with normalized floor heave resulting from panel 1 excavation.

Parameter	Value	Standard Error	t-Value	Probability > |*t*|
Intercept	0.89274	0.05245	17.02098	2.65968E-16
Sandstone thickness	−0.00617	0.00312	−1.97558	0.05813
Distance of sandstone above coal	0.00891	0.00283	3.14537	0.00391
Pillar width	−0.01641	0.00112	−14.6888	1.10111E-14

Adjusted r-square value is 0.87964.

where

SS_thick = stiff sandstone thickness, m
Dist_SS = distance of the sandstone unit above the coal seam, m
Pillar_width = pillar width, m (either 20 or 50 m)

A quantity of interest is the amount of pillar strain, specifically average pillar strain is associated with each case and any relationship between that and the volume of floor heave. Pillar strain was computationally intensive because it required matching up pairs of nodes and tracking their displacement difference, finding that average, and dividing by the original seam thickness.

As results of strain were compiled, the great difference in strain between pillars in some cases was evident. Therefore, the authors decided to represent this difference as a ratio of the absolute value of the average strain of pillar 1 to the absolute value of the average strain of pillar 2. The numerator and denominator are chosen so that the ratio is greater than 1. The results of strain and pillar strain ratios are listed in Table 7. Normalized floor heave and pillar strain ratio are plotted against each other in Figure 4. The correlation is visibly apparent, although it may have a couple of outliers. The fitted linear relationship has an adjusted r-square value of 0.737. The fitted equation is

$$\textit{Normalized floor heave} = 1.01118 - 0.36296 * \textit{pillar strain ratio} \quad \text{(Eq. 2)}$$

Alternatively, we can fit a two-term exponential equation to be

$$\textit{Normalized floor heave} = -0.8194 + 0.54122\, e^{(-psr/0.94335)} + 1.8577\, ee^{(-psr/0.94321)} \quad \text{(Eq. 3)}$$

where

psr = average pillar strain ratio
adjusted r-square value = 0.877

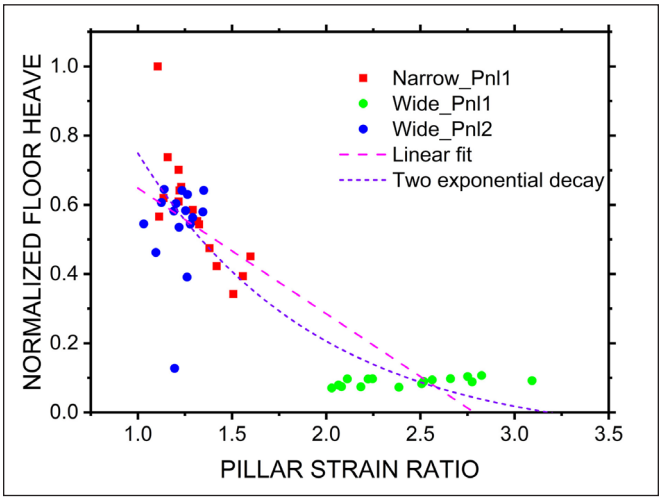

Figure 4. Plot of normalized floor heave ratio versus pillar strain ratio.

Both of these fits are shown in Figure 4.

This equation and Figure 4 demonstrate that floor heave increases when the strains of both pillars are closer to being equal than when they are significantly different. That deduction can be made, even if the panel 2 data is removed from consideration so that only the results of one panel extraction are compared.

The question then becomes what causes a larger pillar strain ratio: What model parameters cause one pillar to strain more than the other? To answer that question, all model parameters identified earlier were used in a multiple linear regression analysis. The adjusted r-square value was 0.89095, and the results are found in Table 8. Sandstone thickness, interface friction, and sandstone modulus

Table 7. Average pillar strains and average pillar strain ratios.

Case	Narrow Panel 1 South Pillar Micro-Strain	Narrow Panel 1 North Pillar Micro-Strain	Narrow Panel 1 Pillar Strain Ratio	Wide Panel 1 South Pillar Micro-Strain	Wide Panel 1 North Pillar Micro-Strain	Wide Panel 1 Pillar Strain Ratio	Wide Panel 2 South Pillar Micro-Strain	Wide Panel 2 North Pillar Micro-Strain	Wide Panel 2 Pillar Strain Ratio
1	−9628.57	−15387.5	1.5981	−4475.19	−1626.75	2.7510	−9879.42	−7320.57	1.3495
2	−18763.9	−22922.9	1.2216	−3011.70	−1425.91	2.1121	−7440.92	−7217.14	1.0310
3	−15778.6	−19193.4	1.2164	−3063.04	−1363.93	2.2457	−7867.64	−6995.18	1.1247
4	−17475.7	−19317.3	1.1054	−2433.75	−1178.40	2.0653	−7620.79	−6340.02	1.2020
5	−18539.3	−21480.1	1.1586	−3084.70	−1292.83	2.3860	−8264.27	−7252.00	1.1396
6	−18666.8	−21216.0	1.1366	−2584.79	−1241.93	2.0813	−7138.52	−5528.86	1.2911
7	−23875.0	−30843.5	1.2919	−4199.09	−1513.27	2.7748	−8362.80	−6860.55	1.2190
8	−9668.63	−13716.0	1.4186	−3851.34	−1502.86	2.5627	−8095.13	−6016.95	1.3454
9	−11120.8	−14741.6	1.3256	−2585.02	−1183.62	2.1840	−7271.25	−6636.51	1.0956
10	−8388.55	−13066.8	1.5577	−3601.77	−1164.53	3.0929	−5082.52	−4252.97	1.1951
11	−17035.7	−22412.7	1.3156	−3349.45	−1335.98	2.5071	−9339.81	−7566.33	1.2344
12	−18718.3	−23035.7	1.2307	−4062.52	−1437.94	2.8252	−8364.91	−6543.84	1.2783
13	−11383.5	−15714.2	1.3804	−3429.77	−1289.44	2.6599	−8852.29	−7061.50	1.2536
14	−18579.2	−22599.4	1.2164	−4113.71	−1633.68	2.5181	−7343.69	−5823.21	1.2611
15	−6658.88	−10034.5	1.5069	−2635.72	−1298.55	2.0297	−8707.33	−7310.45	1.1911
16	−14696.3	−16362.8	1.1134	−2983.86	−1342.39	2.2228	−8438.84	−6679.36	1.2634

Table 8. Results of multiple linear regression analysis of model parameters contributing to pillar strain ratio caused by panel 1 extraction.

Parameter	Value	Standard Error	t-Value	Probability > |*t*|
Intercept	1.25658	0.42106	2.98431	0.00627
Sandstone thickness	0.00212	0.00686	0.30927	0.75968
Interface friction angle	−0.00687	0.00658	−1.04413	0.30642
Sandstone modulus	4.98938E-6	3.06505E-6	1.62783	0.1161
Rest of strata modulus	−1.29403E-5	3.9362E-6	−3.28751	0.003
Distance of sandstone above coal	−0.01351	0.00622	−2.17403	0.03938
Pillar width	0.03797	0.00245	15.48873	2.53631E-14

appear to not be significant factors. Therefore, a subsequent analysis was conducted without those parameters. The adjusted r-square value was 0.88769, and the results are found in Table 9.

The pillar strain ratio, then, significantly correlates positively with pillar width and negatively with the rest of the strata elastic modulus and the distance of the stiff sandstone member above the coal seam. The equation is

$$\begin{aligned} \textit{Pillar strain ratio} = {} & 1.14578 \\ & - 0.0000129403 * \textit{Rest of strata modulus} \\ & - 0.01351 * \textit{SS\_distance} \\ & + 0.03797 * \textit{pillar\_width} \end{aligned} \quad \text{(Eq. 4)}$$

The second two parameters correlated significantly with normalized volume of floor heave. Sandstone thickness was only marginally significant there. The rest of strata modulus makes sense because its stiffness would correlate negatively with the ability of the cantilevered overburden to apply a nonuniform average strain between the pillars.

DISCUSSION

This study has limitations that prevent it from being general in its applicable scope. The model was simplified so that only the coal and immediate floor included the Cavehoek constitutive model, and the rest of the stratigraphy only consisted of a sandstone and one other material, each represented with a strain-softening, ubiquitous joint material to take advantage of the initial sedimentary caving model developed by Itasca (Pierce and Board 2010a, 2010b). Stratigraphy will almost always be more complicated. In addition, more studies should be accomplished to explore the effect of

Table 9. Results of multiple linear regression analysis of significant parameters affecting pillar strain ratio caused by panel 1 extraction.

Parameter	Value	Standard Error	t-Value	Probability > |*t*|
Intercept	1.14578	0.1892	6.05579	1.57521E-6
Rest of strata modulus	−1.29403E-5	3.99451E-6	−3.23952	0.00308
Distance of sandstone above coal	−0.01351	0.00631	−2.14229	0.04101
Pillar width	0.03797	0.00249	15.26264	4.2253E-15

Table 10. List of results from narrow pillar cases 6 and 11.

Parameter	Case 6	Case 11	Percentage Change of Case 11 with Respect to Case 6
Average of pillar microstrains	−19941.4	−19724.2	−1.089%
Pillar strain ratio	1.1366	1.3156	15.76%
Normalized floor heave volume	0.66999	0.49525	−26.08%

material properties chosen for the Cavehoek materials and the effect of various combinations of horizontal stress on floor heave.

This study is important because it included material models that more closely follow caving behavior for sedimentary rock. One could argue for a change in some of the material properties used or for a more realistic (more complicated) geologic column. Despite limitations, the results suggest that even loading or straining of pillars is a condition that increases the volume of floor heave and that floor heave increases with distance between the coal seam and a stiff sandstone member above the coal seam, but decreases with increasing pillar width. The authors' explanation of this phenomena is that more distance allows more even straining of the pillars. However, the authors acknowledge observations that indicate just the opposite effect (D. Su to M. K. Larson, personal communication, February 6, 2020). A combination of Equations 2 or 3 with Equation 4 also suggests that floor heave volume increases with increasing modulus of overburden strata other than sandstone, but this study assumes this strata to be one material. The observation that floor heave volume negatively correlates with pillar width is contrary to the authors' observations at the western U.S. coal mine (Larson, Tesarik, and Johnson, 2020a). However, bands of dissipated plastic energy reached to the middle or just short of the middle of the small pillars, indicating these were near critical pillars. The larger pillars' bands of dissipated plastic energy did not come close to reaching the middle of the pillar, thus indicating that these were abutment pillars. Floor heave in entries between abutment pillars would intuitively be smaller than that in entries between critical pillars. Perhaps that situation had other contributing conditions that overcame the effect of pillar width. The caving conditions did vary at the field site, but the reasons were not sufficiently identified to perform any correlation analyses.

The results suggest that approximately even loading between pillars provides driving forces from both sides of the middle entry to increase floor heave volume. Uneven pillar strains suggests that uneven loading of pillars does not provide as much driving confinement so that floor heave volume is decreased for an equivalent amount of average pillar strain. Although this assertion may not be universally true, and the 16 cases do not provide sufficient opportunities for comparison, one reasonable comparison can be made with the narrow pillar cases of 11 with respect to 6, listed in Table 10. Although the average pillar strains of case 11 are just over 1% less than case 6, the pillar strain ratio and normalized floor heave volume are nearly 16% greater and 26% less for case 11 with respect to case 6, agreeing with the negative correlation between pillar strain ratio and normalized floor heave volume.

CONCLUSIONS

The study described in this paper uses a simple stratigraphy model using state-of-the-art caving constitutive models to determine the correlation of various parameters to floor heave volume. The results show that, for the range of cases used, the normalized floor heave volume correlated positively with distance from the coal seam to a stiff sandstone unit in the overburden; however, this goes against an observation communicated to the authors. Normalized floor heave volume correlated negatively with pillar width, although only two pillar widths were tested in the models. Normalized pillar width correlated negatively with average pillar strain ratio, which is the ratio of average strains in the two pillars, chosen such that the ratio is 1 or larger. This average pillar strain ratio correlates positively with pillar width and negatively with strata modulus other than sandstone and distance of the sandstone unit above the coal seam. The relationship between average strain ratio and normalized floor heave volume appears to be better described by a nonlinear equation, as suggested by the fitted two-term exponential Equation 3.

Further studies should determine the effect of various caving conditions on the amount of floor heave and further explore the effect of pillar width, including documenting the type of pillar—critical, yield, or abutment. In addition, verification with field case studies would strengthen any conclusions.

Even though further study is needed, these results, particularly as shown in Figure 4, imply that floor heave might be minimized by gate road layout design. These preliminary results suggest that if the design of gate road pillars can avoid pillar strain ratios close to 1.0, the risk of floor heave might be decreased. However, the experience of the field study that inspired the current study suggests that the range of conditions at a mine site needs to be well characterized, with caving characteristics having high importance. Such characterization along with further studies would help increase the confidence in a gate road design in minimizing the risk of floor heave.

DISCLAIMER

The findings and conclusions in this paper are those of the authors and do not necessarily represent the official position of the National Institute for Occupational Safety and Health, Centers for Disease Control and Prevention. Mention of any company or product does not constitute endorsement by NIOSH.

ACKNOWLEDGMENTS

The authors thank Daniel Su and Shawn Boltz for their helpful reviews, which strengthened this paper.

REFERENCES

Agapito, J.F.T., Gilbride, L., and Koontz, W. (2005). "Implication of highly anisotropic horizontal stresses on entry stability at the West Elk Mine, Somerset, Colorado." In: Peng, S.S., et al., Eds., *Proceedings: 24th International Conference on Ground Control in Mining*. Littleton, Colorado: SME, pp. 196–202.

Alejano, L.R., and Alonso, E. (2005). "Considerations of the dilatancy angle in rocks and rock masses." *International Journal of Rock Mechanics and Mining Science* 42(4):481–507.

Board, M., and Pierce, M.E. (2009). "A review of recent experience in modeling of caving." In: Esterhuizen, G.S., et al., Eds., *Proceedings of the International Workshop on Numerical Modeling for Underground Mine Excavation Design*. NIOSH Information Circular 9512. Pittsburgh, PA: U.S. Department of Health and Human Services, National Institute for Occupational Safety and Health (NIOSH), pp. 19–28.

Garza-Cruz, T., Pierce, M., and Lavoie, T. (2012). *Implementation of the CaveHoek Constitutive Model within the Longwall Modelling Environment (LME)*. Contract Report ICG10-2552-05-21TM-A. Minneapolis, MN: Itasca Consulting Group Inc.

Harr, M.E. (1987). *Reliability-Based Design in Civil Engineering*. New York: McGraw-Hill.

Hoek, E., Carranza-Torres, C., and Corkum, B. (2002). "Hoek-Brown failure criterion—2002 edition." In: Hammah, R., et al., Eds., *Proceedings of the 5th North American Rock Mechanics Symposium and the 17th Tunnelling Association of Canada Conference: NARMS-TAC 2002—Mining and Tunnelling Innovation and Opportunity*. Toronto, ON: University of Toronto, pp. 267–273.

Itasca. (2009). *FLAC3D: Fast Lagrangian Analysis of Continua in 3 Dimensions—User's Guide, Version 4.0*. Minneapolis, MN: Itasca Consulting Group, Inc.

Kaiser, P.K., and Kim, B.-H. (2015). "Characterization of strength of intact brittle rock considering confinement-dependent failure processes." *Rock Mechanics and Rock Engineering* 48(1): 107–119.

Kim, B.-H., and Larson, M.K. (2019). "Numerical investigation of factors involved in a floor heave mechanism in a bump-prone coal mine." In: Klemetti, T., et al. Eds., *Proceedings of the 38th International Conference on Ground Control in Mining*. Englewood, CO: SME, pp. 93–101.

Kim, B.-H., Larson, M.K., and Lawson, H.E. (2018a). "Applying robust design to study the effects of stratigraphic characteristics on brittle failure and bump potential in a coal mine." *International Journal of Mining Science and Technology* 28(1):137–144.

Kim, B.-H., Pierce, M.E., and Dzik, E.J. (2014). "Numerical investigation of rock mass behavior associated with confinement-dependent strength in brittle failing rocks." In: Labuz, J.F., et al. Eds., *Proceedings of the 48th US Rock Mechanics/Geomechanics Symposium.* Alexandria, VA: American Rock Mechanics Association (ARMA).

Kim, B.-H., Walton, G., Larson, M.K., and Berry, S. (2018b). "Experimental study on the confinement-dependent characteristics of a Utah coal considering the anisotropy by cleats." *International Journal of Rock Mechanics and Mining Science* 105:182–191.

Kim, B.H., and Larson, M.K. (2017). "Evaluation of bumps-prone potential regarding the spatial characteristics of cleat in coal pillars under highly stressed ground conditions." In: *Proceedings, 51st U.S. Rock Mechanics/Geomechanics Symposium.* Alexandria, VA: American Rock Mechanics Association (ARMA).

Kim, B.H., and Larson, M.K. (2018). "Experimental and numerical investigation of the engineering properties of a Utah coal considering the effect of anisotropy due to cleats." In: Schultz, R., Dershowitz, B., and Felice, C., Eds., *ARMA 2018: 52nd US Rock Mechanics/Geomechanics Symposium*. Alexandria, VA: American Rock Mechanics Association (ARMA).

Larson, M.K., and Whyatt, J.K. (2012). "Load transfer distance calibration of a coal panel scale model: A case study." In: Barczak, T., et al., Eds., *Proceedings of the 31st International Conference on Ground Control in Mining*. Englewood, CO: SME, pp. 195–205.

Larson, M.K., Tesarik, D.R., and Johnson, J.C. NIOSH (National Institute for Occupational Safety and Health). (2020a). *Ground stress in mining (part 1): Measurements and observations at two western U.S. longwall mines*. By Larson MK, Lawson HE, Zahl EG, Jones TH. Publication No. 2020–103 (RI 9702). Spokane, WA: U.S. Department of Health and Human Services, Centers for Disease Control and Prevention, National Institute for Occupational Safety and Health, DHHS (NIOSH), 155 pp.

Larson MK, Tesarik DR, Johnson JC NIOSH (National Institute for Occupational Safety and Health). (2020b). *Ground stress in mining (part 2): Calibrating and verifying longwall stress models*. By. Publication No. 2020–104 (RI 9703). Spokane, WA: U.S. Department of Health and Human Services, Centers for Disease Control and Prevention, National Institute for Occupational Safety and Health, DHHS (NIOSH), 257 pp.

Phadke, M.S. (1989). *Quality Engineering Using Robust Design*. Englewood Cliffs, NJ: Prentice Hall.

Pierce, M., and Board, M. (2010a). *Development of a Three-Dimensional Numerical Modeling Environment for Caving and Stress Analysis of Longwall Mining*. Report 2552-05, Prepared for NIOSH, Spokane Research Laboratory. Minneapolis, MN.

Pierce, M., and Board, M. (2010b). *FLAC3D Longwall Modeling Environment*, version 1.0. Minneapolis, MN: Itasca Consulting Group, Inc.

Taguchi, G. (1986). *Introduction to Quality Engineering: Designing Quality into Products and Processes*. Tokyo: Asian Productivity Organization.